

See discussions, stats, and author profiles for this publication at: <https://www.researchgate.net/publication/6433101>

# Molecular simulations bring new insights into flavonoid/quercetinase interaction modes

ARTICLE *in* PROTEINS STRUCTURE FUNCTION AND BIOINFORMATICS · JUNE 2007

Impact Factor: 2.63 · DOI: 10.1002/prot.21380 · Source: PubMed

---

CITATIONS

9

---

READS

68

4 AUTHORS, INCLUDING:



**Sebastien Fiorucci**

University of Nice-Sophia Antipolis

28 PUBLICATIONS 279 CITATIONS

SEE PROFILE



**Jérôme Golebiowski**

University of Nice-Sophia Antipolis

50 PUBLICATIONS 341 CITATIONS

SEE PROFILE



**Serge Antonczak**

University of Nice-Sophia Antipolis

44 PUBLICATIONS 750 CITATIONS

SEE PROFILE

# Molecular Simulations Bring New Insights Into Flavonoid/Quercetinase Interaction Modes

Sébastien Fiorucci, Jérôme Golebiowski, Daniel Cabrol-Bass, and Serge Antonczak\*

Laboratoire de Chimie des Molécules Bioactives et des Arômes, UMR-CNRS 6001, Faculté des Sciences, Université de Nice-Sophia Antipolis, 06108 Nice Cedex 2, France

**ABSTRACT** Molecular dynamics simulations, using the AMBER force field, were performed to study Quercetin 2,3-Dioxygenase enzyme (Quercetinase or 2,3QD). We have analyzed the structural modifications of the active site and of the linker region between the native enzyme and the enzyme-substrate complex. New structural informations, such as an allosteric effect in the presence of the substrate, as well as description of the enzyme-substrate interactions and values of binding free energies were brought out. All these results confirm the idea that the linker encloses the substrate in the active site and also enlighten the recognition role of the substrate B-ring by the enzyme. Moreover, a specific interaction scheme has been proposed to explain the relative degradation rate of various flavonoid compounds under the oxygenolysis reaction catalyzed by the Quercetin 2,3-Dioxygenase enzyme. *Proteins* 2007;67:961–970. © 2007 Wiley-Liss, Inc.

**Key words:** quercetinase; molecular dynamics; structural analysis; enzyme-substrate interactions

## INTRODUCTION

For molecules belonging to the flavonoid family, diversity is the watchword. These compounds can either act as antioxydant, prooxydant, or even as inhibitor, depending on their reacting cofactors.<sup>1–3</sup> Flavonoids are generally involved in biological processes implying ROS or RNS (Reactive Oxygen/Nitrogen Species). Throughout all these reactions, the flavonoids reactive functional group may be different and can then lead to different degradation pathways. Quercetin 2,3-Dioxygenase, an enzyme belonging to the cupin family,<sup>4,5</sup> catalyzes the oxygenolysis of the so-called quercetin flavonoid and leads to the formation of its depside associated to a release of carbon monoxide (Scheme 1). 2,3QD is the only firmly established noniron dioxygenase for which the crystal structure is characterized<sup>6,7</sup> and for which the activity relies on a mononuclear type 2 copper centre.<sup>6–8</sup>

Identifications by X-ray diffraction techniques of the three-dimensional structures for the native enzyme and the enzyme-substrate complex (denoted E/S) have

revealed a homo-dimeric structure. The 2,3QD monomer is composed of two similar domains, both containing hydrophobic cavities, connected together by a flexible linker loop. (Fig. 1) The N-terminal domain hosts the catalytic site, contrarily to the C-terminal domain that lacks a metal centre. In the native structure, the copper ion is mainly coordinated by three histidine residues and a water molecule. A glutamate side-chain, located close to the metal centre, could additionally coordinate the copper cation, but its main role consists in the deprotonation of the C<sub>3</sub>–OH flavonoid function, leading to an enhanced binding of the substrate to the metal. Previous theoretical investigations have revealed that an electron transfer from the flavonoid to the copper atom activates the substrate and favors dioxygen addition.<sup>9,10</sup>

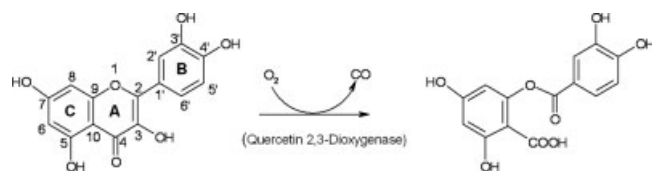
In enzyme catalyzed mechanisms, recognition of the substrate is crucial to obtain a good reaction rate together with a well defined selectivity. In an effort to analyze in details the interaction between the enzyme and the quercetin substrate, Molecular dynamics (MD) simulations have been carried out. Although structural and mechanistic aspects have been tackled in recent studies based on crystallographic data and molecular modeling,<sup>11</sup> the mechanism underlying the substrate recognition as well as the nature of the atoms involved in the first step of the chemical reaction remain a topic of debate.<sup>9,10</sup> In the present study, are exposed some new structural investigations concerning the native and complexed enzymes explored by means of molecular dynamic simulations. On the basis of these structural considerations, a discussion is provided concerning the molecular recognition potencies of 2,3QD towards ligands belonging to the flavonoid family. Such a dynamic behavior analysis will be helpful to give a streamline to the understanding of molecular interactions underlying molecular biology of catalytic enzymes.

The Supplementary Material referred to in this article can be found at <http://www.interscience.wiley.com/jpages/0887-3585/suppmat/>

\*Correspondence to: Serge Antonczak, Laboratoire de Chimie des Molécules Bioactives et des Arômes, UMR-CNRS 6001, Faculté des Sciences, Université de Nice-Sophia Antipolis, 06108 Nice Cedex 2, France. E-mail: Serge.Antonczak@unice.fr

Received 14 June 2006; Revised 28 October 2006; Accepted 22 December 2006

Published online 20 March 2007 in Wiley InterScience (www.interscience.wiley.com). DOI: 10.1002/prot.21380



Scheme 1. Oxygenolysis reaction scheme of quercetin by quercetinase enzyme.

## MATERIALS AND METHODS

### Definition of the System

Starting structures were built using B-chains of experimental X-ray data proposed in the Protein Data Bank (PDB id: 1JUH and 1H1I for the substrate free enzyme and the enzyme-substrate complex, respectively). Since positions of residues numbered from 155 to 163 (1JUH) and from 157 to 158 (1H1I) were not defined in the X-ray structures, they have been added and relaxed using the LEAP module of the AMBER<sup>12</sup> program. Water molecules initially present in the active site have been kept in the structures: 8 in the case of the substrate-free enzyme and 2 when the enzyme-substrate complex was considered. The systems have been neutralized by addition of 17 Na<sup>+</sup> counter-ions placed in the most negative region of space using the LEAP module. Each system has been embedded in a periodic box containing 17183 and 17319 TIP3P water molecules for the substrate-free and for the enzyme-substrate systems, respectively. The water phase was then extended to a distance of 15 Å from any solute atom.

### Copper and Quercetin Parameters

It has been shown that quercetin is oxidized when bound to the metal centre of the active site.<sup>9</sup> Two different oxidation states are thus necessary to describe the copper cation: +II when the substrate is absent and +I when quercetin is found in the structure. The metal centre has been considered as a cation and no bond restraint was applied between the copper and the ligands. van der Waals parameters for Cu(II) were found in forcefields associated with the AMBER program.<sup>13,14</sup> New parameters have been developed for Cu(I) on the basis of results obtained at the B3LYP/6-311+G\* level of computation for four complexes ([Cu(NH<sub>3</sub>)]<sup>+</sup>, [Cu(NH<sub>3</sub>)<sub>2</sub>]<sup>+</sup>, [Cu(NH<sub>3</sub>)<sub>3</sub>]<sup>+</sup>, and [Cu(NH<sub>3</sub>)<sub>3</sub>(HCOO)] considered as models for the residues found in the vicinity of the metal, NH<sub>3</sub> standing for a histidine, and HCOO<sup>-</sup> standing for a glutamate residue. The structures of these complexes have been optimized and the binding energy was further computed, including the Basis Set Superposition Error correction. Then, Molecular mechanics parameters for Cu(+I) have been designed to obtain the best fit with the quantum chemical values, both for the binding energies and the metal-ligand distances. van der Waals parameters have been refined to obtain a good agreement for the binding energy and the metal-ligand distances

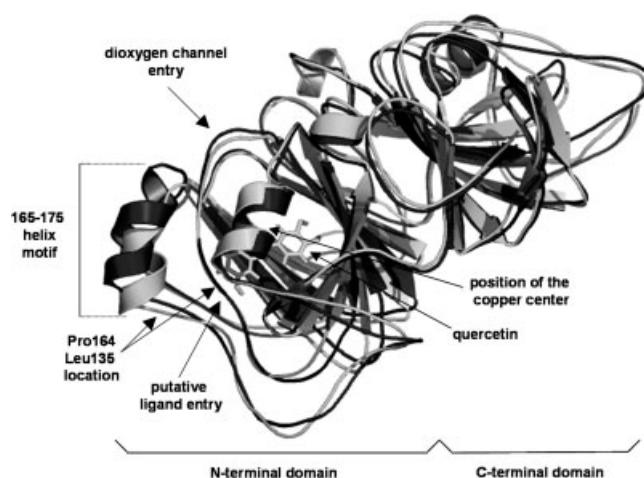


Fig. 1. Superimposed structures of the native protein (dark grey) and the enzyme-substrate complex (light grey) highlighting deformations upon substrate binding. Locations of pertinent residues are indicated (see text).

between the quantum and classical computations. The following parameters can be resumed as: Cu(+I):  $q = +1$ ,  $r_{vdw} = 0.960$ ,  $\epsilon_{vdw} = 0.065$ ; Cu(+II):  $q = +2$ ,  $r_{vdw} = 1.200$ ,  $\epsilon_{vdw} = 0.050$ .

Concerning quercetin, it is assumed that the 3-OH hydroxyl group is deprotonated by Glu73 carboxylate function. Bond, angle, and torsion angle parameters have been assigned on the basis of structures optimised at the B3LYP<sup>15-17</sup>/6-31(+)\*G<sup>18-21</sup> level of theory, using GAUSSIAN98 program.<sup>22</sup> It has previously been shown that such a level of computation reproduces fairly well the structural parameters of similar systems.<sup>9</sup> Atomic charges for the deprotonated oxidized quercetin have been obtained following the RESP charge fitting procedure using B3LYP/6-31(+)\*G\* electrostatic potential. The resulting charges on quercetin are in accordance with those given by others for a similar substrate (kaempferol) bound to 2,3QD, despite the use of different approaches for the description of the electronic structure (see Ref. 11 and Supplementary Material).

### Molecular Dynamics

Simulations were performed using the AMBER6 program and the parm99.dat forcefield. Molecular dynamics (MD) simulations were carried out in the isothermal-isobaric ensemble at 310 K, with the SANDER module using SHAKE on bonds involving hydrogen atoms. A time step of 2 fs was applied. An 8 Å cutoff was applied to nonbonded van der Waals interactions and the non bonded pair list was updated every 25 steps. Once the ions and the water molecules were added to the initial structure, 2000 steps of minimization keeping the solute and the ions fixed, followed by 2000 steps of minimization using particle mesh Ewald (PME) summation and keeping the solvent fixed. The equilibration runs contin-

ued by an equilibration of 50 ps of PME dynamics, keeping the solute fixed. Then, 2000 steps of minimization and 50 ps of MD simulation using a restraint of 30 kcal/(mol Å<sup>2</sup>) on the solute atoms were performed, followed by six rounds of 2000 steps minimization reducing the restraints by 5 kcal/(mol Å<sup>2</sup>) at each round, with 50 ps MD simulation. Further, the system was slowly heated from 100 to 310 K over a period of 20 ps. The equilibration was continued over 50 ps after these 20 ps. Two different simulations noted N1 and N2 in the following, for a total of 6 ns, have been conducted for the native enzyme system, differing only in their initial velocities. Considering the enzyme-substrate (noted E/S) complex, five different simulations, for a total of 11.2 ns have been conducted, differing by the position of the water molecule at the end of the active site and initial velocities. A water molecule is initially present at the cavity end (position 1: between 4'-OH and Thr53; simulations ES1 and ES2). Analysis of the trajectories led us to consider an alternative location for the water molecule (position 2: between both 3'-OH, 4'-OH, and O<sub>Asn74</sub>; simulation ES3) or to consider that it is absent from the binding site (simulations ES4 and ES5). Several simulations were conducted to validate our initial velocities. The initial conditions and the length of each production phase can be found as Supplementary Material.

### Quantum Calculations

In the text, reference is made on free energy barriers computed for the rate limiting step of the oxygenolysis reaction for quercetin, kaempferol, myrecitin, and galangin. These energies have been computed following a methodology presented in Ref. 9, at the B3LYP/6-31(+)G\* level of computation. Furthermore, to assess the role played by amino acids constituting the binding pocket on the substrate, several structures were extracted from the trajectories and relaxed during 2000 steps of minimization. Then, quantum chemical point charge calculations were performed, considering quercetin at the B3LYP/6-31(+)G\* level. Residues constituting the active site (number 33, 35, 51, 52, 53, 63, 67, 69, 73, 74, 75, 112, 123, 132, 135, 136, 139, 163, 169, 172, 175, and 176), the metal centre, and the two water molecules were considered as a background charge distribution. In the quantum chemical calculation, the substrate quercetin was considered as oxidized by the copper cation and deprotonated by GLU<sub>73</sub>. To estimate the polarization effect of water molecules bridging the substrate and amino acids of the cavity, full quantum calculations have been carried out in gas phase on a system made up by quercetin and these water molecules, at the B3LYP/6-31(+)G\* level of computation. None of these model systems is able to reproduce the complexity of the interactions existing within a protein matrix but each of them is able to bring interesting insights on the succession of events that drives the substrate recognition, activation, and degradation during the overall catalytic process.

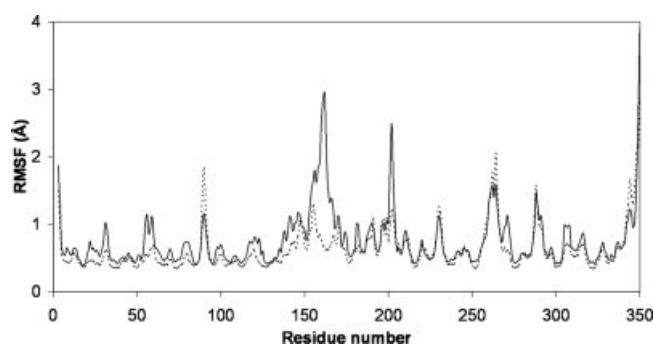


Fig. 2. Root mean square fluctuations of the protein backbone for the native enzyme (solid line) and for the E/S complex (dotted line).

## RESULTS

### Structural Modifications Induced by the Presence of the Substrate

Taking the starting structures as a reference, relatively low root mean square deviations (RMSD < 2.5 Å) along the trajectories are reported, reflecting the stability of the systems during the simulations. Some differences are reported between the systems including or not the substrate. Analysis points out a difference in the structural mobility of the so-called linker region, made up of residues 146–204, linking together the two sub-domains of 2,3QD. Root mean square fluctuations of the linker residues (Fig. 2) show a loss of flexibility for this region in the E/S complex with respect to the free enzyme. This difference in the mobility character for the two systems is in good agreement with the structural indetermination concerning this region, as reported in the X-ray structures. This point is well documented in a previous study devoted to a structural description of the enzyme<sup>11</sup> carried out by molecular simulations. In their study, van den Bosch et al. mainly focused on the specific substrate-linker interactions and on the consequences upon the denaturation of a  $\alpha$ -helix belonging to this linker. Here, as developed below, it is shown that these evolutions in the mobility of the amino acids constituting the linker may play a major role by allowing dioxygen to diffuse into the active site.

A deep analysis of the linker behavior reveals the existence of two sub-units (146–153 and 170–199) present values denoting a typical loop mobility, independently of the presence, or not of a substrate. High differences in the mobility of two other sub-units (154–169 and 200–204) depending on the incorporation of the substrate in the active site are also reported. Residues from 154 to 169 are mobile in the absence of substrate, but the presence of quercetin in the active site diminishes drastically the flexibility of this zone. This trend is also reported for residues 200–204.

Amino acids from 200 to 204 are located close to the second domain of the enzyme and do not interact directly with the substrate. A contrario, amino acids n° 154–164 seem to hold the substrate in the cavity. More specifi-



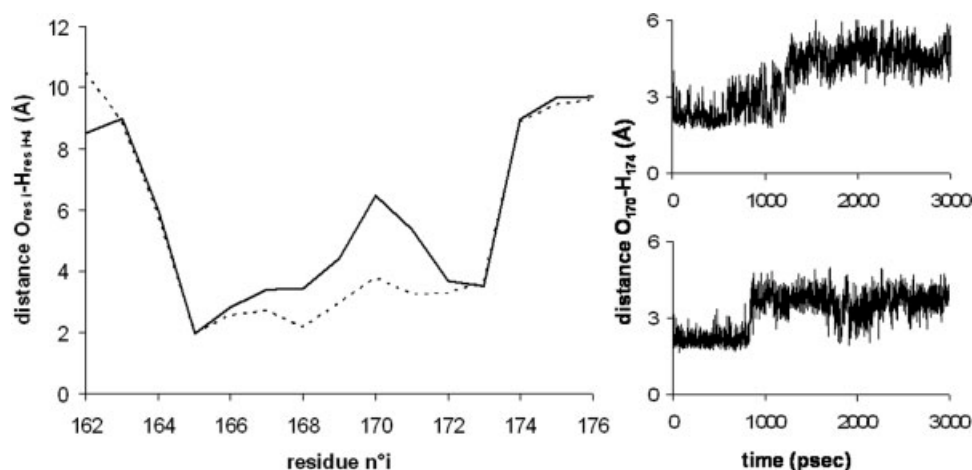


Fig. 3. **a:** Average distance (in Å) between the O backbone atom of the  $i$ th residue and the  $H_N$  backbone atom of the  $(i + 4)$ th residue for the native system (solid line) and for the E/S complex (dotted line); **b:** Evolution of the  $O_i-H(i + 4)$  distance throughout the trajectory between OSer170 and HSer174 for the two N1 (top) and N2 (bottom) native systems.

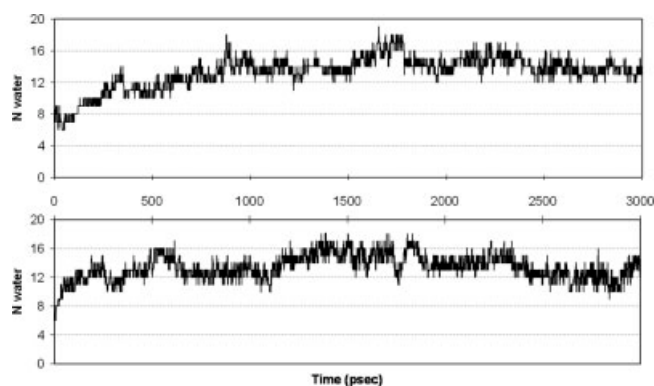


Fig. 4. Number of water molecule (Nwater) versus time (in ps) located in the cavity along two trajectories of the substrate free enzyme.

cally, Pro164 has already been described as the lock of the entry to the active site.<sup>7,11</sup> Here, analysis of the Pro164-Leu139 inter-residue distance, the latter amino acids being located at the opposite side of the cavity entry, highlights the difference between the two systems (complexed or not to the substrate). The average values for this distance are 6.6 and 4.7 Å for the native enzyme and the E/S complex, respectively. This evolution induces a deformation of the  $\alpha$ -helix made up of residues 165–175, as reflected by the distance between the O backbone atom of the  $i^{\text{th}}$  residue and the  $H_N$  backbone atom of the  $(i + 4)^{\text{th}}$  residue (Fig. 3).

However, the average values describing the behavior of the native enzyme have to be considered with care, since two different periods have been identified throughout the trajectory. During these simulations, the number of solvent molecules located in the cavity rises from 8 in the crystal structure to reach an average value of 13–14 (Fig. 4). This result is in good agreement with data previously published,<sup>11</sup> despite differences in the MD protocols used. The authors report that water molecules enter

the cavity to finally reach a number of 13 at the end of their simulation. The same general trend is found in the present analysis. This leads to an increase of the volume in a 700 ps timescale, from 240 Å<sup>3</sup> to a value estimated to 520 Å<sup>3</sup>. Note that the latter value is in good agreement with the 530 Å<sup>3</sup> average volume calculated when quercetin is present in the active site. In their study, van den Bosch et al. have not reported such an evolution. This may come from the methodology they used. Indeed, in their work, the authors have followed the number of water molecules in the cavity along the simulation of a substrate-free enzyme, built from the structure of a substrate/enzyme complex from which the substrate has been deleted.

The deformation of the helix motif involving amino acids from 165 to 175 occurs during approximately the first 1.2 and 0.8 ns of the simulations of the so-called N1 and N2 systems, respectively [Fig. 3(b)]. This period is required to reach a full relaxation of the enzyme, starting from the crystal structure. This point is reflected by evolution of both Ser170-Ser174 and Pro164-Leu139 distances. The first one reflects the deformation of the helix motif while the second reflects the closure of the cavity entry.

A fine analysis of the simulation related to the N1 system puts forward three distinct periods. During the first 600 ps, the Ser170-Ser174 distance oscillates around 2.3 Å, between 600 and 1250 ps this distance shows more important fluctuations around an average value of 2.9 Å and in the last period (from 1250 ps to the end of the simulation) the average value is 4.6 Å. Concerning the N2 system, two periods have been identified. The Ser170-Ser174 distance rises from an average value of 2.6 Å in the first period (from the beginning to 850 ps) to an average value of 3.6 Å in the second period (from 850 ps to the end of the simulation). The two final values are large and thus are not consistent with the presence of a hydrogen bond between Ser170 and Ser174. Never-

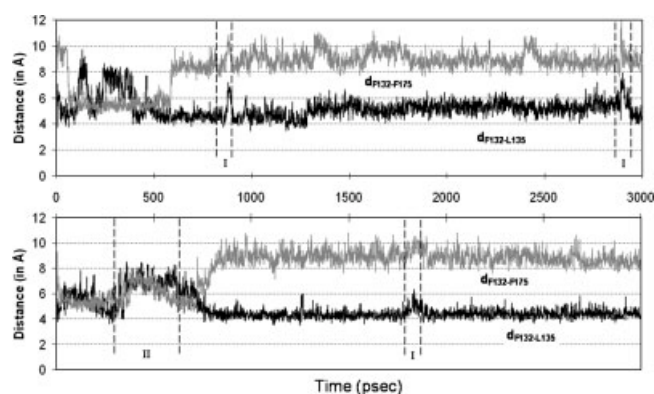


Fig. 5. Distance (in Å) versus time (in ps) between Phe132 and Leu135 and between Phe132 and Phe175 along the two substrate-free simulations (N1 and N2). I and II events are indicated (see text).

theless, the increase of this distance does not lead to a drastic deformation of the  $\alpha$ -helix motif. When the substrate is present in the cavity, fluctuations of this distance are weak and lead to larger average values: 5.4, 6.5, and 5.9 Å for ES1, ES3, and ES4 simulations, respectively. The difference between the values obtained for the native and the complex systems show that introduction of the substrate in the cavity induces an important deformation of the enzyme.

Average values of 7.4, 7.3, and 5.7 Å are found for the Pro164-Leu139 distance in the three successive periods defined in the N1 simulation. Concerning the two periods characterized in the N2 simulation, these average distances are 9.2 and 7.9 Å. Along the simulation of the enzyme-substrate system, a single period is identified and the average value for this distance is : 4.3, 4.3, and 4.1 Å for the ES1, ES3, and ES4 simulations, respectively. It appears then that the cavity entrance is locked by the specific Pro164-Leu139 interaction when the substrate is present in the cavity.

These distances evolve towards the values found in the enzyme-substrate complex but they may never reach these values, since the strong electrostatic interactions between water molecules are likely to prevent the closure of the cavity. More important is that this effect may originate the opening of a channel dedicated to the diffusion of  $O_2$  in the cavity, thus triggering the oxygenolysis reaction. In a previous study,<sup>23</sup> we have shown the existence of such a channel and described the door role played by Phe175. In a first type of event (noted I in Fig. 5) solvent molecules are inserted between Leu135 and Phe132 side-chains and create a chain linking the outer part of the enzyme and the cavity. This is only possible when Phe175 side-chain switches from the enzyme surface to the bulk. In a second type of event (noted II in Fig. 5), water molecules primarily belonging to the cavity diffuse and get inserted between Phe132 and Leu135 amino acids but the connection to the bulk is not possible, since the entrance of channel is locked by Phe175 side-chain. These points are reflected by Phe175-Phe132 distance evolutions plotted on Figure 5. These

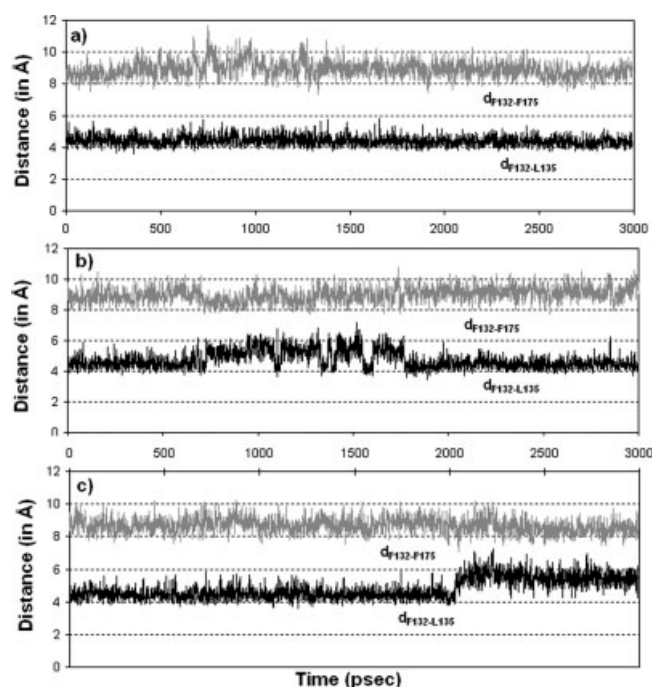


Fig. 6. Distance (in Å) versus time (in ps) between Phe132 and Leu135 and between Phe132 and Phe175 along the three 3 ns long enzyme-substrate simulations (a: ES1, b: ES3, and c: ES4).

two types of events emphasise the door role played by Phe175. Furthermore this channel opening can occur only if the cavity is inflated by a sufficient number of water molecules that is after a 600–700 ps period during which water molecules enter the cavity that leads to inflate the volume and then stretching the linker.

Similar analyses have been carried out for the enzyme-substrate complexes and are presented in Figure 6. On one hand, the large Phe175-Phe132 distances show that the channel is accessible from the bulk from the beginning of the simulations. On the other hand, the values obtained for the Phe132-Leu135 distances are comparable to those found at the end of the N1 and N2 simulations corresponding to the substrate-free systems. This point leads to the conclusion that the opening of the channel does not result from a pure allosteric effect happening only when the substrate is present but also occurs when the cavity is inflated by a sufficient number of water molecules. The crossing of dioxygen through the channel will be nevertheless easier in the absence of hydrophilic molecules in the cavity and can be thus connected to the presence of the substrate. Indeed, dioxygen has not been experimentally detected in the substrate-free enzyme cavity<sup>4</sup> while our results suggest that the channel is in a conformation that should allow a dioxygen molecule to enter the cavity. This point may be rationalized by considering the fact that dioxygen-water interactions do not allow a spontaneous diffusion of  $O_2$  into the cavity. A contrario, when the substrate is embedded in the enzyme, van der Waals type interactions favor the diffusion of  $O_2$  through the channel. In a

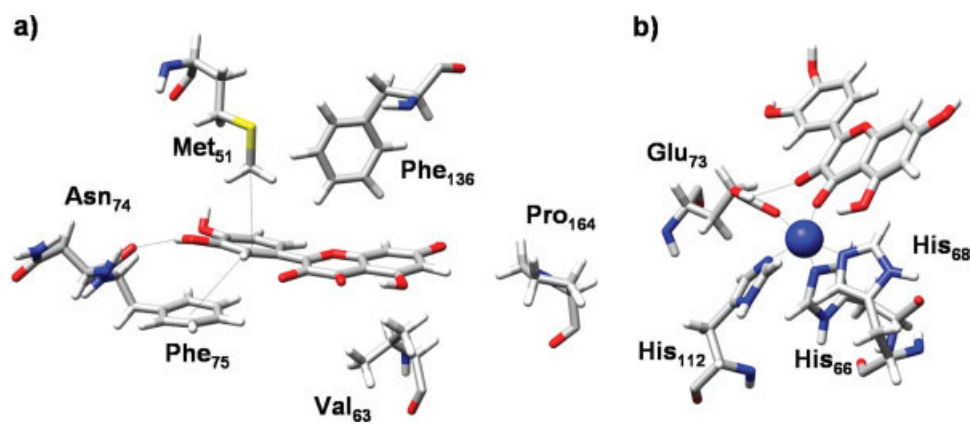


Fig. 7. **a**: Snapshot of the hydrophobic interactions between the substrate and amino acids constituting the inner surface of the cavity; **b**: Snapshot of the first coordination shell around the copper centre.

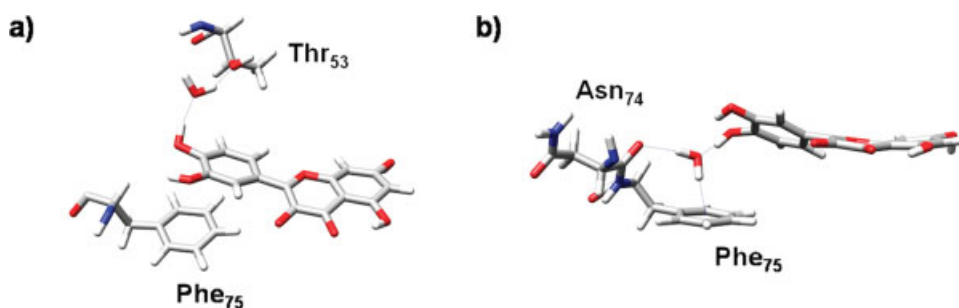


Fig. 8. Alternative positions of the water molecule located at the bottom of the cavity.

previous study,<sup>23</sup> on the basis of the energy profile of O<sub>2</sub> crossing into this channel, we have shown that this process was thermodynamically and kinetically likely to occur.

### Enzyme-Substrate Interactions

Substrate/metal chelation and direct substrate/residues interactions can be decomposed into hydrophobic or hydrophilic components. They originate the activation and recognition processes of the substrate by the enzyme.

Throughout the E/S various trajectories, the metal centre remains tightly bound to the ligands [Fig. 7(b)]. Whatever the simulation considered, Cu-His<sub>66</sub>, Cu-His<sub>68</sub>, and Cu-His<sub>112</sub> average distances are in good agreement with the values given by X-ray structures (about 2.1–2.2 Å for the three ES1, ES3, and ES4 simulations) and the average distance for Cu-Glu<sub>73</sub> is slightly larger than the value obtained experimentally (2.1 Å for the three ES1, ES3, and ES4 simulations versus 1.92 Å in the X-ray structure). The fifth position around the metal centre is occupied by water molecules or by the quercetin flavonoid. Considering the native enzyme simulations, computation of the radial distribution function of the water oxygen atoms around the copper centre shows that two water molecules are at a distance of about 2.0 Å. The

next water molecule is found at an average distance of 4.2 Å. In the enzyme-substrate simulation, quercetin occupies this position in a monodentate way of binding throughout the trajectories. Considering the three ES1, ES3, and ES4 simulations, the average values lie between 2.1 and 2.2 Å for Cu-O3 distance and between 3.6 and 3.8 Å for Cu-O4. In these enzyme-substrate simulations, the copper is modeled as a unitary charge, while quercetin is considered in a semiquinone form and is thus neutral. The system is modeled as to consider that a spontaneous electron transfer from quercetin to the metal center has already occurred. Moreover, copper has been considered as a cation and no bonding term was applied between the metal and quercetin. The consistency of the Cu-quercetin distances throughout the three simulations shows that the parameters we have designed for both the substrate and the metal centre reproduce adequately this Cu<sup>+</sup>-quercetin interaction. As described in the following, this monodentate ligation is partly imposed by interactions between the substrate and amino acids constituting the inner surface of the cavity.

Two water molecules are found in the X-ray structure of the E/S system and are involved in strong enzyme-substrate electrostatic interactions. The first one is found at the entrance of the pocket and creates a bridge through hydrogen bonds between 7-OH<sub>Que</sub> and either OE<sub>Gln33</sub> or OG<sub>Gly62</sub> or also O<sub>Thr162</sub>.<sup>11</sup> This water molecule



is not exchanged with the bulk throughout the simulations and can thus be considered as belonging to the binding cavity. The second water molecule is located at the bottom of the binding pocket. It creates a bridge through hydrogen bonds between O<sub>Asn74</sub> and quercetin O3'H3' and O4'H4' hydroxyl groups. A shift of this water molecule along the simulations led us to consider alternative structures exhibiting hydrogen bonds between O4'H4' and the hydroxyl group of Thr53 (see Figure 8). The third case consists in the deletion of this water molecule from the active site. This leads to the creation of direct hydrogen bonds between both quercetin O3'H3' and O4'H4' hydroxyl group and O<sub>Asn74</sub>. In the two last interaction types, a shift of the substrate is observed towards the bottom of the pocket, leading to a slight shift of the metal centre in the same direction. Nevertheless, the substrate coordination mode on the copper still remains monodentate. These electrostatic interactions participate clearly to the adequate position of the substrate in the active site.

In an effort to gain information on the electrostatic interactions between quercetin and the enzyme, the atomic charges of quercetin have been computed by means of quantum chemical methods, with and without surrounding point charges forming the residues of the 2,3QD binding pocket. The induction effects brought by the binding pocket were deemed rather minor, with charges variations never exceeding 0.04e, except for atoms present in the first coordination sphere of the copper centre. Moreover, full quantum calculations performed in the gas phase on a simple system constituted of quercetin in interaction with one or two water molecules exhibit the same trends. Indeed, no noteworthy polarization of hydroxyl groups to which water molecules are bound, and a fortiori no noteworthy polarization of the delocalized  $\pi$ -systems can be put forward. This confirms that these hydrogen bonds do not play a major role in the polarization of the substrate but, as mentioned in the previous paragraph, these water molecule participate to adequately position the substrate within the cavity.

The cavity of 2,3QD, which is mainly made up of hydrophobic residues, is thus well adapted to molecules belonging to the flavonoid family presenting large  $\pi$ -delocalized rings. Although weak, several interactions are at the origin of the ligand stabilization within the binding pocket. Phe75 and Met51 are in direct interaction with the substrate, and can thus be considered to play a key role in the substrate's recognition by the enzyme [Fig. 7(b)]. The average distances between the mass centre of the carbon atoms constituting the B-ring and the Phe75 side chain are in a 4.3–5.2 Å range. This reflects a  $\pi$ -stacking interaction between the aromatic rings of both residues. On the other hand, the average distances between CE atom of Met51 and B-ring mass centre are in the 3.6–3.8 Å range, reflecting a  $\sigma$ - $\pi$  interaction between the methyl group of Met51 and the aromatic ring of quercetin. Others weak interactions occur between quercetin and residues belonging to the active site, such as a T-shape interaction between Phe136 and

**TABLE I. Substrate Binding Free Energy and Hydration Contribution (in kcal mol<sup>-1</sup>) Calculated for the Five Different E/S Simulations**

	$\Delta G$	Hydration contribution
ES1	-39.4	-6.9 (17.6%)
ES2	-38.6	-7.0 (18.1%)
ES3	-38.1	-8.9 (23.4%)
ES4	-35.4	-2.7 (7.7%)
ES5	-36.0	-2.8 (7.8%)

the A-ring and a  $\sigma$ - $\pi$  interaction between Val63 and the C-ring, as depicted in Figure 7(a).

All these hydrophilic and hydrophobic interactions play a crucial role in the recognition and stabilization processes of 2,3QD for quercetin. Although weak, they can originate a sufficiently efficient interaction, able to discriminate between several species belonging to the flavonoid family. To get insight into the strength of these interactions and to quantify the affinity of 2,3QD for quercetin, binding free energies have been computed considering the E/S trajectories. Energetic analysis has been performed in the presence of water molecules located in the active site. The receptor has been considered either as the protein with the two water molecules or as the lone protein. These two approaches lead to an estimation of the cavity microsolvation contribution to the binding free energy (Table I).

The binding free energy is quite high in absolute value and reveals that quercetin is strongly bound to 2,3QD prior the chemical reaction to occur. The value is consistent throughout the five MD runs and oscillates between -35.4 and -39.4 kcal mol<sup>-1</sup>. Note that the solvation contribution is significant, representing ~20% of the total binding free energy. This contribution becomes weaker than 10% if the water molecule at the end of the active site is removed. Also, the hydration contribution value is higher if the water molecule is positioned between quercetin and Thr53 (ES3), than if it is between quercetin and Asn74 (ES1 and ES2), although the binding free energy is roughly identical.

### Influence of the Substrate Structure on the Degradation Rate

Inspection of the literature reveals that other flavonoids, whose structural difference with quercetin only concerns the number of hydroxyl groups linked to the B-ring, are known to be degraded by 2,3QD with different reaction rates (Fig. 9).<sup>11,24</sup> To estimate if this difference in the substitution plays a major role on the free energy barriers, stationary points of the potential energy surface for the oxygenolysis mechanism have been characterized considering quercetin, kaempferol, myricetin, and galangin flavonoids. These quantum chemical calculations have been performed in vacuum on an isolated semiquinone flavonoid, following the procedure exposed in Ref. 9. They thus can not lead to conclusions on the direct influence of the enzyme on the



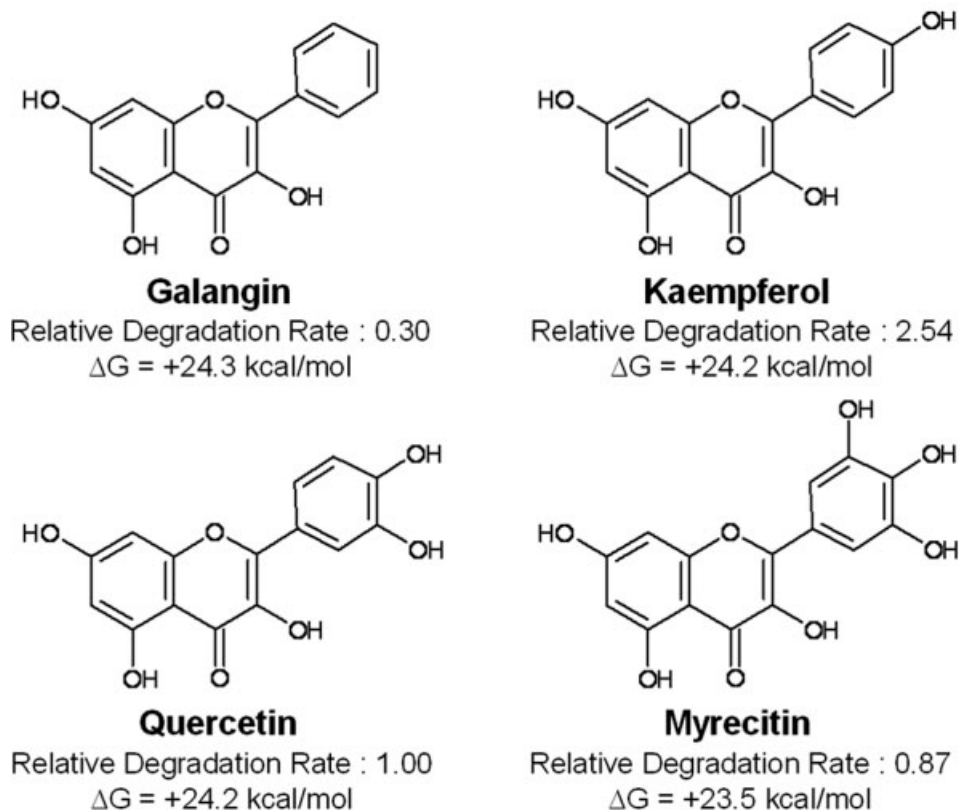


Fig. 9. Relative degradation rate<sup>11</sup> (quercetin is considered as the reference) and calculated free energies for the rate limiting step of the oxygenolysis reaction (following procedure found in Ref. 9) for four flavonoids.

reaction mechanism. However, a systematic study of the influence of the substitution on electronic structures and reaction energies will be of great help in the deciphering of the role of the enzyme in the recognition and activation processes.

The mechanism consists in four successive steps, the first one concerns addition of O<sub>2</sub> on the C2 carbon atom, the second corresponds to the closure of the endoperoxide intermediate. In the two last steps, bonds are broken to produce the depside and carbon monoxide. The same trends are found for the four substrates. Addition of dioxygen on the C2 atom (step 1) is associated to a pyramidalization at the C2 carbon atom and to a rotation of the B-ring with respect to the conjugated A-C rings. The second step is the rate limiting one and the free energy barriers characterized for the four flavonoids are very close, reaching about 24 kcal mol<sup>-1</sup> (Fig. 9). Differences in the values are not significant enough to be exploited to rationalize the nonlinear evolution of the degradation rate. Moreover, the relatively high energy value is expected to be lowered by taking into account the whole environment.

## DISCUSSION

On the basis of these results and the knowledge of the detailed oxygenolysis mechanisms,<sup>9,10</sup> the activation and

the recognition/stabilization processes of the quercetin substrate in the active site of the 2,3QD enzyme appear to be closely connected. Mechanistic studies on model systems have shown that O<sub>2</sub> could be added to the substrate following two different mechanisms. On one hand, dioxygen is first complexed on the metal centre prior to reaction with quercetin. On the other hand, the substrate reacts directly with O<sub>2</sub> through an addition on the flavonoid C2 atom. Both hypotheses have already been explored by means of quantum chemical calculations. These studies did not take into account the steric hindrance, neither the electrostatic field created by the enzyme but only considered the reaction with the metal centre. For a chemical reaction catalysed by an enzyme, the detailed knowledge of the substrate environment and its evolution in time are critical points to understand how the enzyme modulates the potential energy surface of the reaction process.

From this present study, we have learned that quercetin is strongly stabilized in the binding pocket by various types of interactions. The strongest electrostatic interaction that is chelation of the substrate to the metal centre, can be viewed as belonging to the activation process but also can be considered as taking part to the binding of the substrate into the enzyme. Indeed, the binding energy of a deprotonated quercetin onto a naked Cu(+II) is calculated by DFT methods to -508.0 kcal

$\text{mol}^{-1}$ . This ligation is accompanied by an electron transfer from the substrate to the copper and the calculated binding energy of this oxidized substrate with the naked  $\text{Cu}(+\text{I})$  cation remains large:  $-78.8 \text{ kcal mol}^{-1}$ . This result therefore puts forward the importance of both electrostatic and non-additive (charge transfer, polarization) interactions in such complexes. Such effects cannot be reproduced with standard pairwise additive potential and justify efforts to provide a combined analysis by both molecular and quantum mechanics methods. As exposed in the Material and Methods section, the forcefield parameters used for quercetin and for the copper centre take into account this electron transfer from the substrate to the metal. Charges applied on each atomic centre reflect the polarization induced by this ligation.

The presence of two water molecules in the cavity leads to the creation of bridged hydrogen bonds between quercetin and amino acids of the enzyme that stabilize the substrate into the cavity. Our simulations have shown that the active site can adapt to the absence of the water molecule at the cavity bottom. Indeed, despite a slight shift of the metal centre, the substrate remains tightly bound in a monodentate way to the copper cation. These three strong electrostatic substrate/enzyme interactions, metal binding, and H-bondings with water molecules, seem crucial to keep the structural integrity of the reacting system. They can then be described as anchoring points necessary for the substrate to be adequately placed in the cavity of the enzyme. These effects should keep the ligand in the active site for the oxygenolysis reaction to proceed and also to be activated through electron transfer towards the metal centre.

Indeed, our simulations put forward that the presence of the substrate in the active site of the enzyme leads to the opening of a channel that may be dedicated to the diffusion of  $\text{O}_2$  into the cavity.<sup>23</sup> This allosteric effect is triggered by the stretching of the linker that occurs when the cavity volume inflates in the presence of water molecules or in the presence of the substrate. More generally, the importance of the role of linkers has been reported in a recent article.<sup>25</sup> In our previous study,<sup>23</sup> we have shown that this channel points directly towards the quercetin  $\text{C}_2$  carbon atom. Hence, it can be postulated that the role of the linker is dual: first, it closes the entry dedicated to the substrate (as reflected by the Pro164-Leu139 distance) that locks the flavonoid into the cavity, as reported previously<sup>11</sup>; second, it opens a new access dedicated to  $\text{O}_2$  that is the third protagonist of the oxygenolysis reaction.

In this biomolecular system, numerous interactions are rather hydrophobic, such as the stacking of  $\pi$  rings for instance, and each of them plays a role in the stabilization of the substrate in the enzyme. But here again, it appears that the interactions driven by the amino acids constituting the binding pocket can also play a major role in the activation of the substrate. Indeed, dioxygen addition onto quercetin is favored when the substrate is pyramidalised at the  $\text{C}_2$  carbon atom.<sup>9</sup> This pyramidalization is accompanied by a rotation of the catechol group

leading to a non planar configuration of the substrate. Analysis of our simulations leads to average values of  $(0 \pm 10)^\circ$  for the pyramidalization and  $(0 \pm 15)^\circ$  for the rotation (torsion angle:  $\text{C}3\text{C}2\text{C}1'\text{C}2'$ ) at this carbon atom. These fluctuations are induced by amino acids movements constituting the binding pocket, such as Met51 and Phe75 for example, that push up and down the rings of quercetin around the three anchoring points described above. Quantum calculations have estimated to about  $0.1 \text{ kcal mol}^{-1}$  the energy needed for a  $10^\circ$  rotation of the catechol group and to about  $2.5 \text{ kcal mol}^{-1}$  the energy needed for a  $15^\circ$  pyramidalization at the  $\text{C}_2$  carbon atom. Though planar in its most stable conformation, quercetin has been found in a bent conformation in the X-ray structure<sup>7</sup> and our quantum calculations show the feasibility of a limited deformation of the quercetin structure. By these two types of deformations, quercetin adapts to the fluctuations of the surrounding amino acids and always exhibits the best interaction scheme with the enzyme and is prepared to the addition of dioxygen at the  $\text{C}_2$  carbon atom.

The degree of functionalization of the flavonoid involved in the reaction process implying 2,3QD plays a crucial role on the contribution of both hydrophobic and hydrophilic part throughout the recognition process by the enzyme. Other flavonoids, whose difference with quercetin is only the number of hydroxyl groups bonded to the structure, such as kaempferol, galangin, and myricetin, are known to be degraded by 2,3QD with different reaction rates (Fig. 7).<sup>11,24</sup> Quantum chemical calculations performed in the absence of the enzyme have shown that the number of hydroxyl groups has no influence on the barrier heights of the rate limiting step of the reaction. They thus only influence the substrate recognition prior the reaction to occur. The difference in their reaction rates then appears to be due to the presence of hydroxyl groups at given positions. All these flavonoids present the same A and C-ring and only differ by their substitution on the B-ring.

The degradation rate does not follow the number of hydroxyl groups present on the substrate. Kaempferol is the best substrate for Quercetin 2,3-Dioxygenase enzyme although its number of hydroxyl groups is between those of quercetin and galangin. It follows that some of these hydroxyl groups may act as recognition amplifiers and other may not. The only hydroxyl functional group on the B-ring involved in the enzyme-substrate interaction is found on the 4' position ( $\text{O}4'\text{H}4'$ ). This position interacts with a water molecule located at the bottom of the binding pocket. The remainder of the substrate is likely to perform the same interaction as described with quercetin. Hence, this suggests that this 4' hydroxyl group is crucial for ligand recognition but also for substrate activation. Also, other hydroxyl groups (3' and 5') tend to lower the affinity of 2,3QD for the substrate. On the basis of results discussed earlier, it can be postulated that these additional hydroxyl groups, through interactions with the surrounding amino acids, prevent a totally free rotation/pyramidalization around  $\text{C}_2$  carbon

atom that could prepare the substrate for dioxygen addition. A contrario, absence of hydroxyl group at the B-ring leads to a lack of an anchoring point and then to a bad position of the substrate within the cavity.

The determination of the dynamic behavior of such biomolecular systems might help in the understanding of their chemical reactivity. To this end, the results of theoretical simulations, as those carried out in this work, will be extremely useful.

## CONCLUSION

Incorporation and stabilization of a substrate into an enzyme is highly dependent on recognition processes of the active molecule by residues constituting the binding pocket, but it is also known that allosteric effects driven by the substrate onto the enzyme structure may be crucial for the catalyzed reaction to proceed. Here, our MD simulations have put forward that a combination of these two effects exists in the flavonoid/2,3QD system. Indeed, when the substrate is located in the active site, a stretching of the so-called linker region contributes to lock the flavonoid into the cavity but also gives rise to the opening of a dioxygen channel allowing the oxygenolysis reaction to proceed.

Furthermore, recognition and activation of flavonoids in Quercetin 2,3 Dioxygenase enzyme appears to be a subtle balance between substrate/enzyme hydrophobic and electrostatic interactions. On the basis of the present results, it seems difficult to attribute a simple role for each of the amino acids constituting the active site. Generally speaking it appears that the interactions that underlie the recognition and stabilization processes of the substrate in the binding pocket also play a non-negligible role in the activation of this molecule.

## ACKNOWLEDGMENTS

The authors greatly acknowledge the CMIM (Centre de Modélisation et d'Imagerie Moléculaire) of the University of Nice and the CINES (Centre Informatique National de l'Enseignement Supérieur) for provision of computation time. The reviewers are greatly acknowledged for interesting comments.

## REFERENCES

- Cotelle N. Role of flavonoids in oxidative stress. *Curr Top Med Chem* 2001;1:569–590.
- Jovanovic SV, Steenken S, Tosic M, Marjanovic B, Simic MG. Flavonoids as antioxidants. *J Am Chem Soc* 1994;116:4846–4851.
- Nagao A, Seki M, Kobayashi H. Inhibition of xanthine oxidase by flavonoids. *Biosci Biotechnol Biochem* 1999;63:1787–1790.
- Fusetti F, Schröter KH, Steiner RA, van Noort PI, Pijning T, Rozboom HJ, Kelk KH, Egmond MR, Dijkstra BW. Crystal structure of the copper-containing quercetin 2–3-dioxygenase from *Aspergillus japonicus*. *Structure* 2002;10:259–268.
- Dunwell JM, Khuri S, Gane PJ. Microbial relatives of the seed storage proteins of higher plants: conservation of structure and diversification of function during evolution of the cupin superfamily. *Microbiol Mol Biol Rev* 2000;64:153–179.
- Hund HK, Breuer J, Lingens F, Huttermann J, Kappl R, Fetzner S. Flavonol 2,4-dioxygenase from *Aspergillus niger* DSM 821, a type 2 CuII-containing glycoprotein. *Eur J Biochem* 1999;263:871–878.
- Steiner RA, Kalk KH, Dijkstra BW. Anaerobic enzyme-substrate structures provide insight into the reaction mechanism of the copper dependent quercetin 2,3-dioxygenase. *Proc Natl Acad Sci* 2002;99:16625–16630.
- Kooter IM, Steiner RA, Dijkstra BW, van Noort PI, Egmond MR, Huber M. Copper-mediated oxygenolysis of flavonols via endoperoxide and dioxetan intermediates. *Eur J Biochem* 2002;12:2971–2979.
- Fiorucci S, Golebiowski J, Cabrol-Bass D, Antonczak S. Oxygenolysis of flavonoid compounds: DFT description of the mechanism for the quercetin case. *Chem Phys Chem* 2004;5:1726–1733.
- Siegbahn PEM. Hybrid DFT study of the mechanism of quercetin 2,3-dioxygenase. *Inorg Chem* 2004;43:5944–5953.
- van den Bosch M, Swart M, van Gusteren WF, Canters GW. Simulation of the substrate cavity dynamics of quercetinase. *J Mol Biol* 2004;344:725–738.
- Pearlman DA, Case DA, Caldwell JW, Ross R, Cheatham TE, III, DeBolt S, Ferguson D, Seibel G, Kollman P. AMBER, a package of computer programs for applying molecular mechanics, normal mode analysis, molecular dynamics and free energy calculations to simulate the structural and energetic properties of molecules. *Comput Phys Commun* 1995;91:1–41.
- De Kerpel JOA, Ryde U. Protein strain in blue copper proteins studied by free energy perturbations. *Proteins* 1996;36:157–174.
- Jorgensen WL, Maxwell DS, Tirado-Rives J. Development and testing of the OPLS all-atom force field on conformational energetics and properties of organic liquids. *J Am Chem Soc* 1996;118:11225–11236.
- Becke AD. Density-functional exchange-energy approximation with correct asymptotic behavior. *Phys Rev A* 1998;38:3098–3100.
- Becke AD. Density-functional thermochemistry. III. The role of the exact exchange *J Chem Phys* 1993;98:5648–5652.
- Lee C, Yang W, Parr RG. Development of the Colle-Salvetti correlation-energy formula into a functional of the electron density. *Phys Rev B* 1988;37:785–789.
- Ditchfield R, Hehre WJ, Pople JA. Self-consistent molecular-orbital methods. IX. An extended Gaussian-type basis for molecular-orbital studies of organic molecules. *J Chem Phys* 1971;54:724–728.
- Hariharan PC, Pople JA. The influence of polarization functions on molecular orbital hydrogenation energies. *Theoret Chimica Acta* 1973;28:213–222.
- Clark T, Chandrasekhar J, Schleyer PvR. Efficient diffuse function-augmented basis sets for anion calculations. III. The 3–21+G basis set for first-row elements, Li–F. *J Comput Chem* 1983;4:294–301.
- Krishnam R, Binkley JS, Seeger R, Pople JA. Self-consistent molecular orbital methods. XX. A basis set for correlated wave functions *J Chem Phys* 1980;72:650–654.
- Frisch MJ, Trucks GW, Schlegel HB, Scuseria GE, Robb MA, Cheeseman JR, Zakrzewski VG, Montgomery JA, Jr, Stratmann RE, Burant JC, Dapprich S, Millam JM, Daniels AD, Kudin KN, Strain MC, Farkas O, Tomasi J, Barone V, Cossi M, Cammi R, Mennucci B, Pomelli C, Adamo C, Clifford S, Ochterski J, Petersson GA, Ayala PY, Cui Q, Morokuma K, Malick DK, Rabuck AD, Raghavachari K, Foresman JB, Cioslowski J, Ortiz JV, Baboul AG, Stefanov BB, Liu G, Liashenko A, Piskorz P, Komaromi I, Gomperts R, Martin RL, Fox DJ, Keith T, Al-Laham MA, Peng CY, Nanayakkara A, Gonzalez C, Challacombe M, Gill PMW, Johnson B, Chen W, Wong MW, Andres JL, Gonzalez C, Head-Gordon M, Replogle ES, Pople JA. Gaussian 98, Revision A. 7, Gaussian, Inc., Pittsburgh, PA, 1998.
- Fiorucci S, Golebiowski J, Cabrol-Bass D, Antonczak S. Molecular simulations reveal a new entry site in quercetin 2,3-dioxygenase. A pathway for dioxygen? *Proteins* 2006;64:845–850.
- Oka T, Simpson FJ, Krishnamurthy HG. Degradation of rutin by *Aspergillus flavus*. Studies of specificity, inhibition and possible reaction mechanism of quercetinase. *Can J Microbiol* 1972;18:493–508.
- Wriggers W, Chakravarty S, Jennings PA. Control of protein functional dynamics by peptide linkers. *Biopolymers* 2005;80:736–746.